

University of South Florida
Development of a Smart Window for Green Buildings in Florida

PI: Dr. Sarath Witanachchi
Students: Marak Merlak, Ph.D

Description: This proposal is aimed at developing a smart window concept that has the potential to convert part of the solar radiation falling on windows during daytime to electricity, and to use this harnessed energy to power a phosphor-based, highly efficient white-light LED source to illuminate the building at night. This project pursues two different technologies: (1) use of quantum dot based solar cells to harvest solar energy, and (2) develop an electroluminescent light source based on nanophosphors to provide illumination for buildings. The proposed work brings together two unique nanoparticle growth techniques developed at the Laboratory for Advanced Material Science and Technology (LAMSAT) at USF to fabricate a prototype device that would demonstrate the possibility of significant energy savings. Research accomplishments related to solar device were presented in last annual report. This report focuses on research developments in the solid state lighting device.

Budget: \$38,413
Universities: USF

Progress Summary

The microwave plasma system was used to grow nanophosphors of La₂O₃:Bi and CaS:Eu. The system was modified to accommodate chemical vapor deposition (CVD) of ZnO and ZnS. ZnO coatings were grown by introducing Zinc acetylacetonate (Zn(acac)₂) vapor as precursor near the substrate. Vapor was generated by heating granules of Zn(acac)₂ in a container to 160^oC and pushing the vapor with gas that contained a mixture of Ar and oxygen. Dimethylzinc and H₂S were used for the growth of ZnS films. A patent application has been filed for this hybrid process for fabricating nanoparticle embedded coatings.

Microwave plasma process allows control of nanophosphor particle sizes by controlling the precursor concentration. We have demonstrated the ability to deposit La₂O₃:Bi nanophosphors in single crystal form with sizes from 5nm to 100 nm by changing the starting concentration. Transmission Electron Microscopy (TEM) images in Fig 6 (a) & (b) show the hexagonal crystals and clear lattice planes with $d=3.34\text{\AA}$ that corresponds to (100) orientation. BTO layer required for the device structure was sputter deposited at low temperature.

Table 1: Integrated Sphere measurements of luminous flux from a 1cmx1cm area of devices.

Color	Conventional Structure	Proposal Structure
Blue	540 μW	720 μW
Red	580 μW	800 μW

Radiant flux emitted by devices fabricated with the conventional EL structures and devices with the proposed structures were measured by the integrated sphere technique. Measured values in μW for emission area of 1cmx1cm from blue and red devices are presented in Table 1 (rounded to the nearest 10s). These values represent average of 5 similar devices. Even though, the absolute values of emission are low, these measurements show an enhancement in emission resulting from the proposed structure. The observed upward trend confirms the viability of the concept and the

potential of EL devices fabricated under optimum conditions to reach desired outputs of 1300-1500 μW (13-15 W/m^2).

Annual Progress Report

Project Description

Project consists of two main research thrusts: (1) develop a PbSe quantum dot (QD) based polymeric solar cell structure as a window film to convert solar radiation through windows to electricity, (2) Develop a electroluminescence-based (EL) solid state lighting device that can be powered by the harnessed solar energy to provide lighting at night. A novel EL device architecture has been investigated in this project. This report describes the results pertaining to the EL device.

Electroluminescence based light sources:

EL occurs when impurity ions in a crystalline phosphor is excited by high-energy electrons. The electronic states of the dopant ions in the host crystal are split by the crystal field energy, which determines the energy levels available for excited electrons. Bound electrons of impurity ions such as Eu^{2+} , Ce^{2+} , Bi^{2+} , Mn^{2+} etc. are excited to higher energy levels when impacted with high-energy free electrons. Spontaneous de-excitation gives rise to optical emission where the emission wavelength is a characteristic of the type of impurity atom and the host material. Any excess energy will also be released to the lattice as a phonon (Fig. 1), which in general is very small. The band gap of the host material has to be larger than the energy of the emitted photon to prevent reabsorption of the radiation. For this mechanism to work there has to be a source of electrons and an externally applied electric field of the order of 10^6 V/cm to accelerate electrons in the conduction band of the host material.

A simple EL device consists of a phosphor layer such as Mn doped ZnS ($\text{ZnS}:\text{Mn}$) that is sandwiched between two insulating layers (Fig. 1).

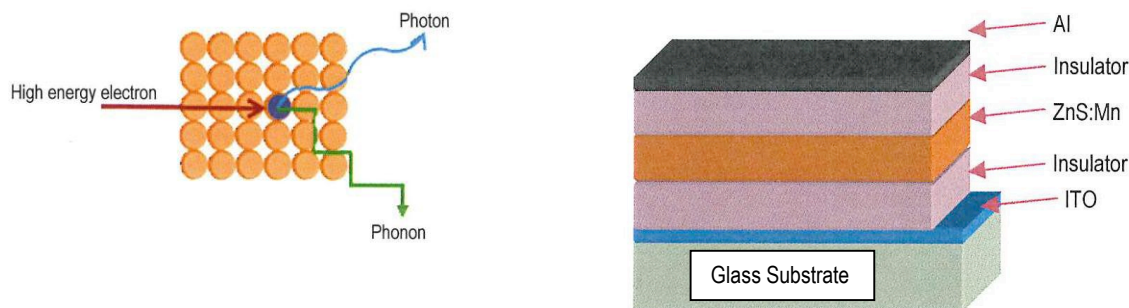


Fig. 1: Mechanism of EL and thin film layered structure of a typical EL device.

One of the electrodes is transparent, such as indium tin oxide (ITO) that allows light to transmit. When a high enough voltage is applied (above a threshold) between the electrodes the localized electrons in the interfacial trap states are injected into the conduction band of ZnS and accelerated by the electric field. These high-energy electrons cause impact excitation of dopants (eg. Mn).

Advantages of EL lights:

Currently available EL lights produce low intensity levels ($70\text{-}300$ Candela/ m^2 , EL Inc.) and thus are limited to special applications. If the light output can be increased, EL lights offer significant advantages as grow-lights for agriculture. These advantages include;

- (1) Emission spectrum from phosphors is much broader than that from an LED chip and thus can create light outputs that can be customized to any color temperature. Almost all of the energy from the electrons is converted to optical radiation. Amount of heat generated is much smaller than in an LED. Not having to incorporate heat management components simplifies the light fixture and reduces the device cost.
- (2) Multiple layers of the device can be manufactured by low-cost techniques such as role-to- role fabrication by inkjet printing or screen-printing. Manufacturing cost is much lower than the epitaxial thin film growth techniques used for fabricating LED chips.
- (3) Currently, a 1.5 m² white light panel can produce about 850 lumens, which is equivalent to a 60W incandescent light bulb. EL light is a thin flexible sheet that illuminates a large area uniformly (Fig. 2). The main advantage offered by an EL light source is that it is an extended source where light propagates in almost planar wave fronts. For such an extended source, the decrease in intensity of light (W/m²) with distance from the source is very small. This is a great advantage for a room lighting in contrast to 1/r² variation produced by a point source such as an **LED**.



Figure 2: EL based light sheet.

Function of Phosphors:

Phosphors are oxide, nitride, or sulfide host materials that carry small percentage of (~1%) impurity ions (Ce, Eu, Tb, Mn, Cu, Ag, Pb, Bi) as active ions. The crystal field energy of the host structure causes the splitting of the energy level in the active ions leading to an absorption line in blue and emission lines at longer wavelengths with long lifetimes (phosphorescence). Hundreds of phosphor materials with emission from deep blue to deep red have been synthesized. Some of the well known phosphor materials include, Ce^{3+} and/or Eu^{2+} doped $\text{Y}_3\text{Al}_5\text{O}_{12}$ (YAG: $\text{Ce}^{3+}, \text{Eu}^{2+}$), $\text{Y}_2\text{O}_3:\text{Eu}^{2+}$, $\text{Ba}_3\text{MgSi}_2\text{O}_8:\text{Eu}^{2+}$, Mn^{2+} , $\text{ZnS}:\text{Mn}$, $\text{CaS}:\text{Cu}$, $\text{CaS}:\text{Pb}^{2+}$, $\text{CaS}:\text{Eu}^{2+}$.

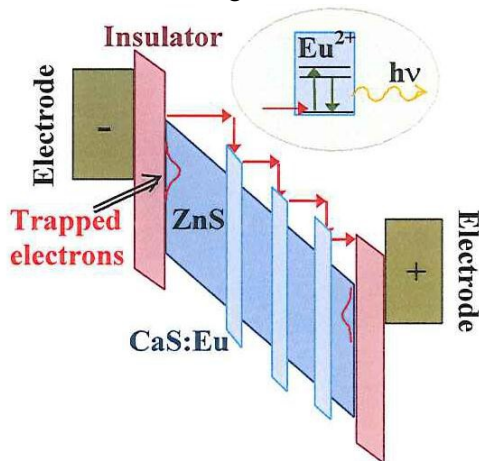


Fig. 3: Band alignment of an EL device structure that is subjected to an external voltage. Inset shows the photon emission from the impurity ion.

Advantages of nanophosphors:

Conventional phosphor materials fabricated by solid state sintering methods are in micrometer scale and thus light scattering at grain boundaries is significant. Light scattering reduces the extraction efficiency of the source. When the phosphor particle size is few tens of nanometers, much smaller than the wavelength of light (400-800 nm), effect of light scattering is significantly reduced. The Mie scattering cross-section of particles below 50nm is very small. In addition, when the phosphor particle size is reduced to the scale of tens of nanometers, the surface area-to-volume ratio of the material is increased, leading to an increase in the luminous efficiency.

The following factors determine (limit) the maximum emission produced by currently available nanophosphor based EL device:

- (1) Electrons required for excitation are derived from trap states at the insulator-host interface. In presence of a high AC voltage (100-200V) they are released from traps (Poole-Frenkel effect) and accelerated in the conduction band of the semiconductor host (Fig. 3). Under the AC field, electrons oscillate between the two sides to generate photons. Higher the voltage higher the emission.
- (2) Emission lifetime of a phosphor (decay time τ) is a characteristic of the host and the impurity. Typical lifetimes are in the range of 1 μ seconds to 100's of milliseconds. The driving frequency should be less than $1/\tau$ to avoid phosphor saturation. Currently devices are operated at about 600 Hz. As the phosphor particle sizes are reduced into the nanometer region, modification of the crystal field of the phosphor host (CaS in CaS:Eu) causes the decay time to be smaller and thus enable high frequency operation.

(3) Higher voltages and frequencies produce higher emission, but at the expense of reduced device lifetime. For low duty cycles, the device may last forever. However, in continuous use at high power outputs, the intensity drops with time and may need replacement in 2-3 years.

Experiments and Results:

The microwave plasma system for nanoparticle growth consist of three main regions; (1) nebulizer to for 1-1.5 μm aerosol droplets of the precursor, (2) plasma reaction zone where microwave energy generates a high temperature reaction zone for evaporation of the solvents and reaction of the chemicals in droplets and plasma gas to form the nanophosphors, (3) substrate placed above the plasma zone for the deposition of the nanophosphors. The system was modified to accommodate chemical vapor deposition (CVD) of ZnO and ZnS. ZnO coatings were grown by introducing Zinc acetylacetonate ($\text{Zn}(\text{acac})_2$) vapor as precursor near the substrate. Vapor was generated by heating granules of $\text{Zn}(\text{acac})_2$ in a container to 160°C and pushing the vapor with gas that contained a mixture of Ar and oxygen. Dimethylzinc and H_2S were used for the growth of ZnS films. For safe handling of the chemicals involved, the entire system was placed in a fume hood (Fig. 4). A patent application has been filed for this hybrid process for fabricating nanoparticle embedded coatings.



Fig. 4: Picture of the microwave plasma system used in the growth of nanophosphors, ZnO and ZnS layers.

Step 1: The starting point in the fabrication of the layered structure is a commercially available ITO (layer 1) coated glass substrate. The choice of the insulator (layer 2) was BaTiO_3 (BTO) (refractive index (n) = 2.01). BTO and n-ZnO (n = 2.0) films were deposited by sputtering.

Step 2: ZnO films were also grown by the CVD process within the microwave plasma system on sputtered BTO films. Growth by CVD is much simpler and cost effective than sputtering. ZnS films were deposited by CVD process with Dimethylzinc and H_2S gas.

Step 3: The two phosphor materials to be used to generate blue and red radiation are $\text{La}_2\text{O}_3:\text{Bi}$ (blue) and $\text{CaS}:\text{Eu}^{2+}$ (red), respectively. $\text{La}_2\text{O}_3:\text{Bi}$ nanoparticles were grown by the microwave plasma process with starting precursors containing aqueous solutions of the nitrates of La and Bi salts. Depending on the starting concentration, particles of sizes from 5nm to 100 nm were deposited. $\text{CaS}:\text{Eu}$ nanophosphor coatings were grown in two steps. In the first step, $\text{CaS}:\text{Eu}$ nanoparticles of sizes of about 50 nm were grown by solvothermal process. Subsequently, particles were dispersed in ethanol and nebulized in the microwave plasma system to deposit a coating on a substrate. Layers of ZnS and ZnO were grown by the same method used in step 2.

Microwave plasma process allows control of nanophosphor particle sizes by controlling the precursor concentration. We have demonstrated the ability to deposit $\text{La}_2\text{O}_3:\text{Bi}$ nanophosphors in single crystal form with sizes from 5nm to 100 nm by changing the starting concentration. Transmission Electron Microscopy (TEM) images in Fig 5 (a) & (b) show the hexagonal crystals and clear lattice

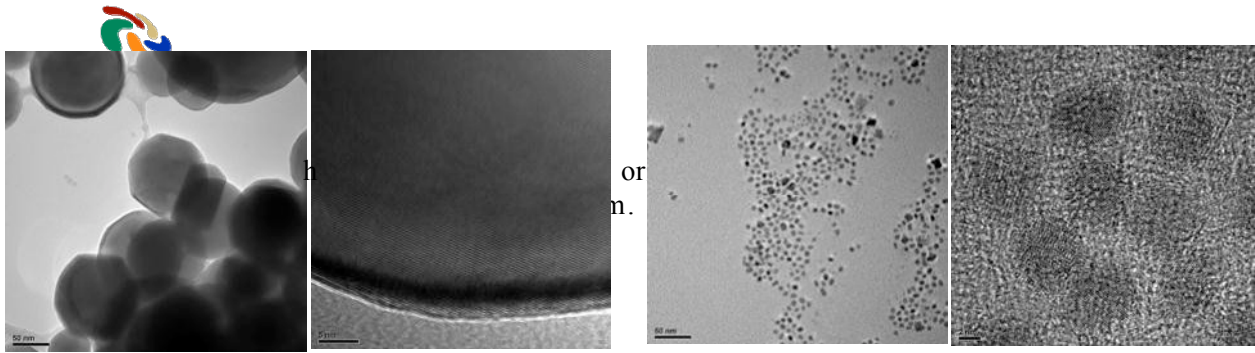


Fig. 5: TEM images of La₂O₃:Bi nanophosphors by microwave plasma process for, (a) 0.1M solution, showing 50-75 nm particles, (b) lattice planes at high resolution indicating single crystal nature, (c) 0.01M solution, particle sizes of 5-6 nm, (d) lattice planes at high resolution.

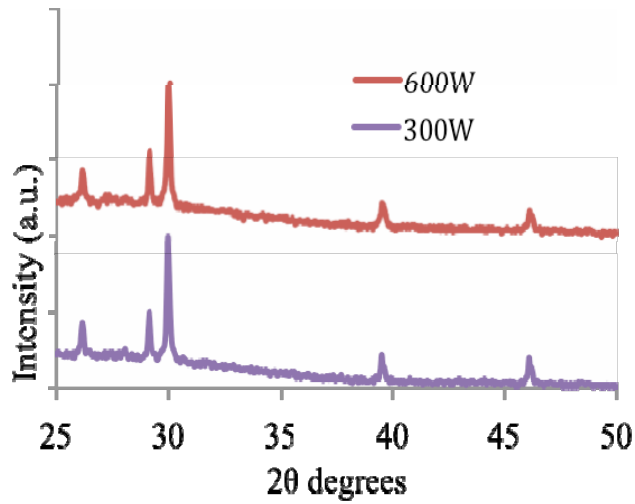


Fig: 6: XRD patterns of as-deposited La₂O₃:Bi³⁺ nanophosphor coatings at two different power levels indicating crystallinity.

Step 4: BTO layer was sputtered at low temperature. Silver ink was used as the back electrode.

Each coating was analyzed by x- ray diffraction for crystallinity and absorption spectroscopy for light transmission. Fig. 6 shows x-ray scans of nanoparticle coatings grown under two different microwave powers. In addition to the n-ZnO/p-ZnS p-n junction structure, n-ZnO-p-NiO junctions were also investigated. Since one of the blue phosphors under consideration is La₂O₃:Bi, possibility of embedding oxide phosphor in a p-type oxide semiconductor rather than ZnS was explored.

Light output measurements: One of the devices fabricated by steps outlined above and the observed blue and red emission from these devices are shown in Fig. 7. Radiant flux emitted by devices fabricated with the conventional EL structures and devices with the proposed structures were measured by the integrated sphere technique. Measured values in μW for emission area of 1cmx1cm form blue and red devices are presented in Table 1 (rounded to the nearest 10s).

Table 1: Integrated Sphere measurements of luminous flux from a 1cmx1cm area of devices.

Color	Conventional Structure	Proposed Structure
Blue	540 μW	720 μW
Red	580 μW	800 μW

These values represent average of 5 similar devices. Even though, the absolute values of emission are low, these measurements show an enhancement in emission resulting from the proposed structure. The observed upward trend confirms the viability of the concept and the potential of EL devices fabricated under optimum conditions to reach desired outputs of 1300-1500 μW (13-15 W/m²).



Fig. 7: (a) View of a device fabricated with nanoparticle coatings, (b) blue emitting device with La₂O₃:Bi phosphor, (c) red emitting device with CaS:Eu phosphor.